
Article:
Barrie, C. orcid.org/0000-0001-5338-9273, Fernandez-Silva, B. orcid.org/0000-0003-2288-9675, Snell, R. orcid.org/0000-0002-4981-3518 et al. (2 more authors) (2023) AddFAST: A hybrid technique for tailoring microstructures in titanium-titanium composites. Journal of Materials Processing Technology, 315. 117920. ISSN: 0924-0136

https://doi.org/10.1016/j.jmatprotec.2023.117920

Journal of Materials Processing Tech. 315 (2023) 117920

Contents lists available at ScienceDirect

Journal of Materials Processing Tech.

journal homepage: www.elsevier.com/locate/jmatprotec

*Add*FAST: A hybrid technique for tailoring microstructures in titanium-titanium composites

Cameron Barrie *, Beatriz Fernandez-Silva, Rob Snell, Iain Todd, Martin Jackson

Department of Materials Science and Engineering, The University of Sheffield,Mappin Street, Sheffield S1 3JD, UK

ARTICLE INFO

Associate Editor: Adam Thomas Clare

Keywords:
Field-Assisted Sintering Technology
Spark Plasma Sintering
Additive Manufacturing
Titanium alloy
Interpenetrating phase composite
Composite microstructure

ABSTRACT

The advantages of FAST sintering have prompted much process research and application. From this came opportunities to investigate the potential for designing complex interpenetrating microstructures by combining the powder bed with a pre-built solid lattice structure, which bonds with the powder to become one. Producing the lattice structure through Additive Manufacturing yields a columnar grain morphology and texture, contrasting to the powder grains when bonded and creating a controllable composite microstructure of interpenetrating grain types. Here, we demonstrate with Ti-6Al-4V that this *Add*FAST technique successfully creates parts with this complex microstructure. The samples show a precise arrangement of grain sizes and texture with high densification and bonding. This demonstrates the technique's viability and the process parameter values that control the final microstructure, while showing the ability to combine different alloys within the part and to retain microstructural quality in deformation. Verifying this *Add*FAST process creates opportunities to design controlled, complex microstructures in small parts.

1. Introduction

Among the varied sintering processes available for metallic and ceramic parts, Field-Assisted Sintering Technology (FAST – also known as Spark Plasma Sintering) has emerged as an effective technique with several useful advantages. Through the combination of a uniaxial applied force and either a pulsed or continuous electric current, the method can densify a variety of material powders at very high process rates compared to processes like Hot Isostatic Pressing. The current generates Joule heating at points of resistance leading to fast and high-intensity heating, as described by Suárez et al. (2012). Combined with the applied load, this leads to high final densities at shorter densification times than similar technologies, as demonstrated by Eriksson et al. (2005). A schematic diagram of FAST is shown in Fig. 1.

FAST also offers an opportunity as a way to potentially reduce processing costs of difficult-to-manufacture materials like titanium alloys. The cost breakdown of producing titanium parts, as described by Dutta and Froes (2017), shows the major contribution of process energy and inefficiencies to costs. This includes machining 'buy-to-fly' ratios that can cause over 80 % of the titanium stock used to produce components to be machined off and converted to scrap, wasting both material and the energy used in its processing. Powder processing methods like FAST can bypass or reduce several of the expensive thermomechanical processing and machining stages, with FAST's energy-efficiency and short processing times make it especially appealing for this purpose. The rapid heating rates of FAST processing also lead to minimal grain growth and the retention of strong, fine-grained microstructures. Bowden and Peter (2012)'s analysis of the costs of conventional and neat-net shape powder manufacturing of titanium parts shows that even though particle feedstock for FAST is more expensive than mill product, the vastly-superior material efficiency leads to overall cost reductions. Some additional techniques can use FAST to further reduce the material and energy waste of machining, i.e. FAST-*forge*, introduced by Weston and Jackson (2017), in which powder is consolidated in a shaped preform followed by a one-step forging deformation to create the desired near-net-shape part. The preforms are shaped through the FAST technology by graphite moulds. Processes like this can reduce the material and energy waste of the machining stage.

Another benefit of FAST is its effectiveness in creating diffusion bonds during sintering. Interfaces between mixed composition regions sintered by FAST in the appropriate conditions exhibit dense, clear diffusion bonds. Decker et al. (2016) showed bonds of this quality and

* Corresponding author.
E-mail addresses: cgbarrie1@sheffield.ac.uk (C. Barrie), b.silva@sheffield.ac.uk (B. Fernandez-Silva), r.m.snell@sheffield.ac.uk (R. Snell), iain.todd@sheffield.ac.uk (I. Todd), martin.jackson@sheffield.ac.uk (M. Jackson).

https://doi.org/10.1016/j.jmatprotec.2023.117920
Received 31 October 2022; Received in revised form 9 February 2023; Accepted 14 February 2023
Available online 21 February 2023

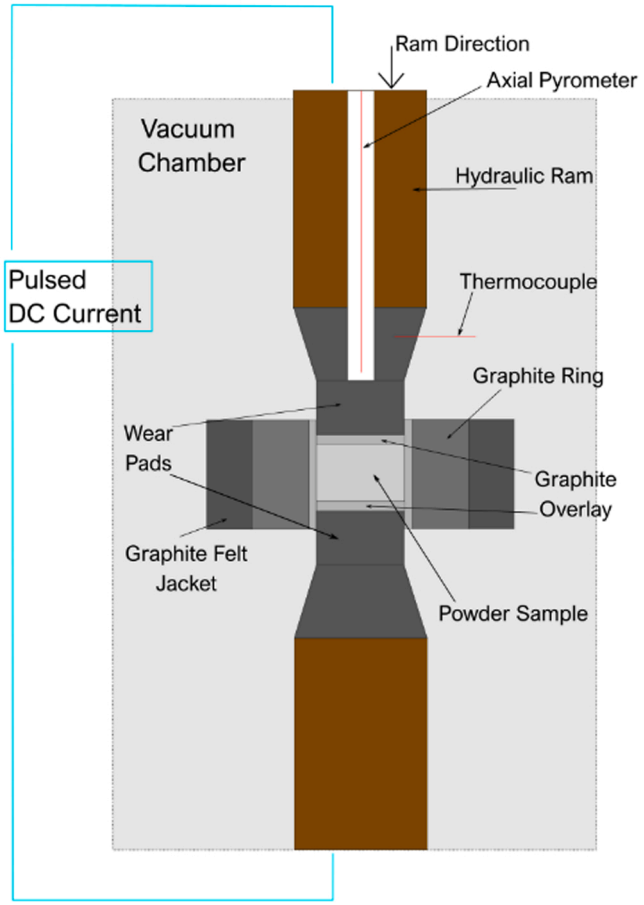

Fig. 1. Schematic diagram of Field-Assisted Sintering Technology.

high part density when sintering Ti-6Al-4V and TiAl powder by FAST. Pope et al. (2019) also showed high-quality bonds and interfaces between regions of CP-Ti, Ti-6–4 and Ti-5–5–5–3 powder in FAST, with some areas showing grains growing across the interface. Their mechanical testing of these samples showed that the join was strong and high-quality, with failure occurring in the surrounding alloy rather than at the bond. He et al. (2012) found that bulk Ti-6–4 interfaces not only bonded well by FAST but also showed grain growth across in the interface, as seen with powders in previously-mentioned work. Quality of bonding, densification and performance is also seen when FAST powders are sintered in the mould with pre-fabricated rods and fibres. Dong et al. (2016) sintered 2024Al powder with TiNi fibres in FAST and produced dense, high-quality metallurgical bonding between the two phases. Kozlík et al. (2021) bonded Ti Grade 2 wire with Al6061 powder and found similar high-quality bonding. This prompts investigation into how the utility of this diffusion bonding strength can be employed. Powder could be bonded to a greater variety of structures than simple rods, ones possessing different grain design or more-complex geometry, to create microstructures or properties unavailable in the powder sintered by itself.

One way to create addition structures of this kind is through additive manufacturing (AM). This group of processes creates a unique opportunity to create extremely fine and detailed structures with far greater ease than subtractive manufacturing, as well as the potential to precisely design and tailor a structure for individual applications. A schematic diagram of the powder-bed AM process is shown in Fig. 2.

AM usage still encounters some significant challenges. The AM process can be very slow to produce objects of meaningful size, as described by Duda and Raghaven (2016), and can easily generate a number of unwanted defects. Gong et al. (2014) varied a range of AM

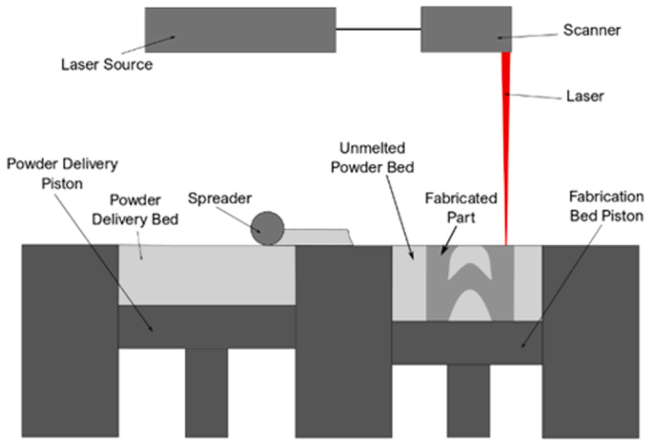

Fig. 2. Schematic diagram of the powder-bed AM method.

process parameters and found that poor value choice in almost all parameters could lead to significant defects. Voids can also be left by poor powder packing, which causes hot tearing if the molten metal fails to fill the gap before it solidifies. Unmelted powder can bond to the edges of the melt pool to create surface satellites (Huang and Yeong, 2018). AM parts are also susceptible to high surface roughness, as the edges of each layer create a step effect (Mumtaz and Hopkinson, 2010). Naturally, these issues have led to a lot of research into ways to rectify these defects. Molaei and Fatemi (2019) showed that re-scanning the build in situ can prove effective, although it can require a lot of process data for suitable results. Post-processing treatments like Hot Isostatic Pressing have also been effective (Al-Bermani et al., 2014), but add further costly steps to a processing method already known to be time-intensive.

Another effect of powder-bed AM processing is the consequences for microstructure. As the area of beam focus is heated intensely from above and surrounded by cooler powder, significant temperature gradients are created in the melt. The result is an environment that encourages vertical grain growth (Wei et al., 2015). This also affects texture, as the orientation of the forming dendrites will be skewed by the grain direction of favourable growth that is closest aligned to the heat flow (Lee et al., 1997). As a result, multiple as-built grains will grow along the same or similar axes, which in the large vertical grains can lead to long regions of consistent texture. Vertical grains, by themselves, are unsuitable for many applications due to their anisotropy and ease of deformation. However, if a part could be fabricated so that varying grain sizes or aligned crystallographic texture existed in a controlled manner in different regions, it could be possible to use AM behaviour to create a complex microstructure of differing microstructural features. Controlling the arrangement of these features may then lead to parts with site-specific or graded properties.

In this paper, we propose a production method – termed *Add*FAST - that incorporates the different technologies AM and FAST to create small titanium parts with tailored microstructures and the potential for novel, controllable properties. Our proposal is that during the lay-up of powder in the FAST mould, small items or structures built by AM could be placed into the mould as well with the loose powder. These would then consolidate by diffusion bonding during the FAST process, joining the two regions together into one hybrid composite. The different structure of each region would combine to create a complex, inter-penetrating microstructure, leading to novel behaviour. The use of AM means that these structures can be designed with high precision and complexity, giving us a great degree of control over their effect on the resulting composite. Lattice designs are particularly interesting for this because their strut arrangement means they possess a large-scale macrostructure, which may allow for more-complex responses that could be adjusted by design as well as being open enough for powder to infiltrate and bond throughout. No melting occurs in FAST, so the architecture of the AM

parts could be retained into the final part and influence further deformation stages. Conversely, the deformation of these stages could deform the lattice into a final configuration or size that it takes throughout the service life. Although numerous conventional designs exist for lattice structures (cubic, octahedral etc.), varying optimisation processes have been developed to create lattices of complex forms for AM that allow them to excel in various attributes. Bi-directional Evolutionary Structural Optimisation has demonstrated ability to self-optimise a starting topology, with the capacity to add and remove material as necessary for optimisation (Querin et al., 2000). The Solid Isotropic Microstructure with Penalty method can achieve optimisation of generalised shapes with high degrees of accuracy to a known design (Rozvany et al., 1992). The Lattice Structure Lightweight Triangulation can match sample geometry in a small, low-computational-requirement number of shapes and elements, allowing efficient processing (Chougrani et al., 2017). Methods such as these have helped develop complex designs such as the triply-periodic minimal surface set of lattices. Gyroid-type triply-period lattices can create a stress distribution that greatly improves lattice properties such as fatigue behaviour (Yang et al., 2021). Design processes for creating effective graded structures have also been demonstrated (Nguyen, 2021); these have been used by Zhang et al. (2022), for graded versions of complex structures like the gyroid triply-period design as well, with improved strength and deformation behaviour. The ability to optimise lattice designs in numerous ways for a suite of desirable properties could make lattices particularly useful as the additions in these samples.

Other potential practical advantage of this process method include the correction of the common defects encountered in AM, as the FAST sintering could close the internal part porosity. The surrounding powder would also cover the naturally-rough AM outer surface. The process described has the potential to be applied to a vast variety of alloy systems, including combining different alloy systems in one part – although titanium has particular potential for use with FAST, there is nothing about this process that inherently requires a particular alloy or composition. A schematic of the process is shown in Fig. 3.

FAST and AM techniques have been used in conjunction in various ways so far. Mostly, this occurs by one technique serving as the focus, while the other acts to improve or benefit the former in some way. As a densification technology, FAST can be used to remove porosity from monolithic AM items - Levy et al. (2018) demonstrate a recent example of this with laminated steel parts. The French company Norimat have filed multiple patents for approaches where a complex-shaped AM item can be densified in FAST by surrounding it with a sacrificial powder in the FAST mould, breaking the powder away after processing (Beynet et al., 2019a) (Beynet et al., 2019b). AM has, likewise, been used to improve FAST operations. Torresani et al. (2023), demonstrate how building a graphite mould by AM allows FAST powder to be sintered into more-complex designs than normally achieved due to the complex mould shape. Norimat have also filed a patent for a process of building a countermould design for FAST by AM that allows complex FAST items to be shaped in the mould, successfully retaining their shape in compression (Beynet et al., 2019c). In comparison, less research has been done on combining a FAST-built part with an AM-built part in one item. Hernández-Nava et al. (2019) sintered AM-built designs with powder in HIP, which created complex grain architecture and altered mechanical properties, and our *Add*FAST process intends to combine this work with the natural advantages of FAST processing. This would allow for utilising the strengths of both FAST and AM in load-bearing parts.

Combining these technologies in ways similar to our intended investigation has received little research attention. Observations on combining powder FAST and AM in this way only go back around half a decade and have primarily focused on using it to create composites that combine material properties. Rahmani et al. worked extensively on this combination of processes in recent years with great success, with two studies on combining a Ti-6–4 lattice with sintered diamond particles to combine the deformation capacity, impact absorption and weldability of Ti with the hardness and wear properties of diamond (Rahmani et al., 2019a) (Rahmani et al., 2019b). They produced similar combinations of Ti's deformability with the wear resistance of WC-Co particles to increase impact absorption of the hardmaterial item (Rahmani et al., 2020). Combining a Ti-6–4 lattice with silver-doped titania by FAST was used to impart strength and damage tolerance to another application where the emphasis was the antibacterial effect of the doped titania (Rahmani et al., 2019c). They also used the combination of a Ti-6–4 lattice and powder by FAST to improve the properties of the Ti structure, such as using wollastonite powder to increase interfacial bonding in biomedical uses (Rahmani et al., 2019d). Reinforcing the Ti-6–4 structure with diamond particles as it was printed allowed it to act as an internal reinforcement to a sintered matrix of Ti-6–4 powder (Rahmani et al., 2019e). In other research centres, Liashenko et al. (2020) used the combination of an AM lattice filled with powder to create a composite of dense (AM) and porous (sintered powder) regions in the part. Diverse and fruitful as these investigations have been, they have all emphasised using the process to create composites that focused on the properties of two different materials. Martin et al. (2016), to the authors' knowledge, represent the only research so far on using this method with a particular interest in the complex microstructure created by the combination of two regions. Their analysis identified the difference in prior β-colony regions between the matrix and lattice areas, as well as the similarity in (α + β) lath microstructure in each area. However, they did not consider potential behaviours that might result from this microstructure or the ways these structures may respond to various stimuli and processing parameter variations; their assessment of performance was chiefly that of microhardness, caused by the difference in composition between areas. This work marks our investigation intended to develop this further to understand the inherent properties, limits, practical requirements and application potential of combining the two regions' differing microstructure through this technique, with the focus of our *Add*FAST process being utilisation of the AM microstructure itself beyond the direct combination of two materials.

2. Methodology

2.1. Materials

The primary material used in these tests was the α + β alloy Ti-6Al-4V (Ti-6–4), although the near-α alloy type Ti-6Al-2Sn-4Zr-2Mo (Ti-6–2–4–2) powder was used in one particular set of samples (as will be discussed in Section 3.4). The titanium alloy system was chosen as a set with particular existing potential for FAST, as mentioned already, and

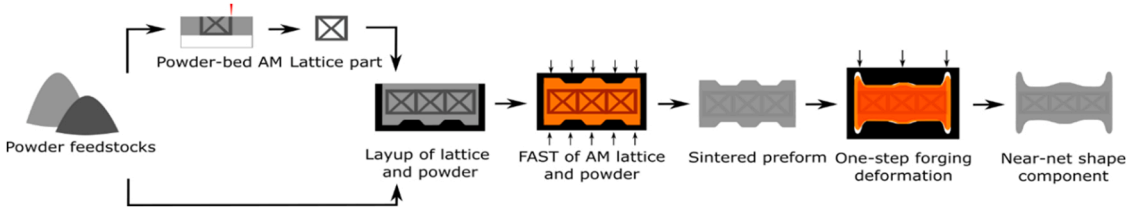

Fig. 3. Schematic diagram of the proposed AddFAST hybrid manufacturing process.

Ti-6–4 was considered the key alloy for this work due to its prevalence in application. Same-alloy pairings in each region of the composite were used for the majority of the work to facilitate analysis of how the process creates a complex microstructure, as well as of its quality. These powders were all prealloyed, had spherical morphologies and were fabricated respectively by Renishaw plc and LPW Technology Ltd. Their particle size distributions are given in Table 1, which were determined using a Malvern Mastersizer 3000 with a wet dispersion method.

2.2. AM structures

2 AM structure designs were used for our addition parts. The first was a diamond cubic lattice with a strut thickness of 1 mm and a relative density of 0.08 (referred to hereafter as the DC lattice). This structure was built as a large lattice, as described in Hernández-Nava et al. (2016), before sectioning into 1 cm cubes with a water jet cutter followed by an Abrasimet 250 with a diamond wafer blade. The second structure design was based on the BCC unit cell converted into struts and consisted of this unit cell repeated twelve times. The second structure was introduced to test application of the process to a fine structure of complex design, based on a well-known lattice structure, as well as being introduced in particular tests as part of an ongoing investigation into the effect of different lattice designs on mechanical properties of *Add*FAST parts. These BCC lattices were built as individual items in an Aconity3D AconityMINI SLM machine with a laser power of 190 W and a speed of 1200 mm/s, using a hatch distance of 80 μm and a layer thickness of 30 μm. Each BCC addition had a height of 8.49 mm, a base edge length of 5.6 mm and a strut thickness of 1 mm. The structure of these designs are shown in Fig. 4. All addition parts were made from Ti-6-4.

2.3. Field assisted sintering and AddFAST

The FAST process was conducted with an FCT Systeme GmbH SPS Furnace Type HP D 25 machine. The machine measured temperature with a vertical pyrometer, positioned 3 mm from the contact surface. These were fed through the hydraulic rams at the top and bottom of the assembly; these were the source of both manual compression and direct electrical current that created the Joule heating. The assembly in the machine consisted of a 20 mm diameter mould, lined inside with graphite foil and wrapped in a graphite felt jacket to reduce heat losses. The rams, ram support wear pads and the wear pad-powder contacts were also lined with graphite discs, as illustrated in Fig. 1. Given the presence of the AM additions, the mass of powder to be used could not (for most samples) be determined directly from the intended final sample volume. Powder mass was instead determined by measuring the mass of a powder batch with a balance, adding an appropriate amount to the mould and then measuring the change in mass. Powder was added by pouring enough to visually obscure the bottom graphite disc, shaking the mould gently to spread the powder evenly, placing the AM structure on top of this powder base, and then pouring powder so as to infiltrate the structure as evenly as possible, until the whole AM structure was visually obscured. Again, the mould was gently shaken to flatten the top surface after pouring.

All FAST samples in this work were processed with an applied pressure of 35 MPa, a heating rate of 100 °C/min and a vacuum environment. Most samples were held for a dwell time of ten minutes; a set of samples were specifically made using longer dwell periods, discussed in Section 3.2. Dwell temperature varied from 850 to 1100 °C between samples, as will also be discussed in Section 3.2. An example of an as-built *Add*FAST sample is shown in Fig. 5.

2.4. Mechanical compression testing

After FAST processing, compression samples were machined out from the 20 mm diameter FAST billet. These were machined to standard ASTM dimensions of 15 mm height, 10 mm diameter, and for *Add*FAST samples were machined to ensure that the AM lattice remained in the centre of the composite part. Axisymmetric compression of the samples was carried out with a purpose-built servo hydraulic-controlled compression machine at the University of Sheffield, as also described in Weston and Jackson (2017). These were performed at room temperature under a constant strain rate of 0.1 s^{-1}.

2.5. Analysis techniques

Sectioning of FAST samples was done along the vertical axis through the flat face of the cylinder, using an Abrasimet 250 and diamond wafer blade. These were then mounted in Bakelite with the through-thickness surface facing up. The mounted samples were polished to P2500 with SiC paper by standard metallographic procedure, followed by polishing with a polishing medium of 0.04–0.06 μm Silico suspended in hydrogen peroxide. Grinding and polishing were carried out on a Tegramin 25 machine.

Light microscopy was conducted on a Nikon ECLIPSE LV150/LV150A microscope, and contrast adjustments (to accentuate microstructural features and boundaries) were done using ImageJ software. All light microscopy images were taken under cross-polarised light. Porosity measurements were determined used a set of five micrographs for each sample, chosen randomly after removing from selection ones that did not show the required microstructural areas. Porosity was measured using threshold measuring in ImageJ. Grain size measurements were performed using the light micrographs by the Linear Intercept Method. Grain texture analysis was performed by Electron Backscattered Diffraction (EBSD) in a JEOL JSM-7900 F SEM equipped with a Symmetry detector and AZtecHKL software for data collection. Low-resolution texture maps were obtained covering areas of $600 \times 450\ \mu m^2$ and $2 \times 4\ mm^2$, using 2 and 5 μm step sizes, respectively. Further post-processing was performed with MTEX open source software (Klein and Schwarzer, 2010) to obtain the orientation maps. IPF (Inverse Pole Figure) orientation maps are plotted regarding the Y direction (which is equivalent to the compression direction during the FAST processing).

3. Results and discussion

3.1. AddFAST microstructure and interface

The *Add*FAST sample sintered at 950 °C with the DC lattice is shown in Fig. 6. The micrographs clearly show two distinct regions of grain structure: one of small, relatively-equiaxed grains and one of large, columnar grains. These two regions are characteristic of post-sintered fine powder and AM structures built under high thermal gradients, respectively. From this, therefore, we see that we have successfully created a contrasting microstructure of interpenetrating grain structures through this method, confirmed by the distinctive grain morphologies of the two regions. The arrangement of the two regions also indicates that the architecture of the AM part's struts is retained into the composite – the regions of large grains form the shape of the AM addition. This

Table 1
Particle size distribution of the powders used this paper.

Material	Dx (10) average (μm)	Dx (50) average (μm)	Dx (90) average (μm)	Relative span average
Ti-6–4	19.5	30	45	0.85
Ti-6–4–2–4	24.4	38.4	58.4	0.89

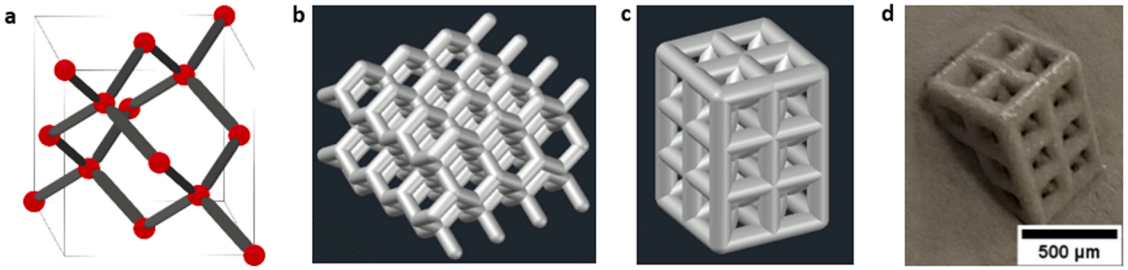

Fig. 4. a. The diamond cubic (DC) lattice used in testing, as a schematic image of the unit cell. b. The DC lattice in AutoCAD. c. The Compound-BCC lattice used in testing in AutoCAD. d. The photograph of Compound-BCC lattice on a bed of powder.

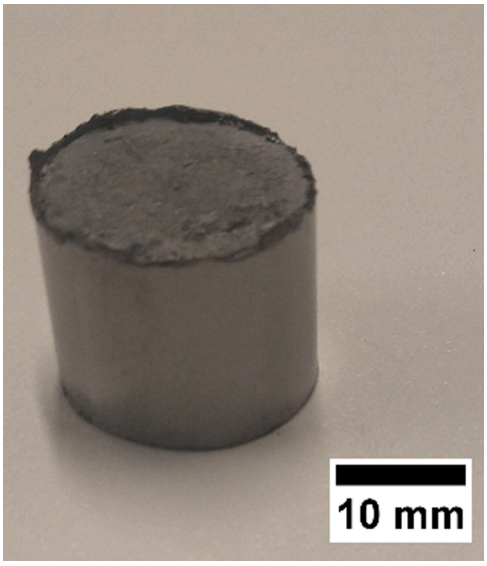

Fig. 5. Photograph of an example of an as-built AddFAST sample.

means that the distribution of these large grains in the composite can be manipulated by altering the design of the original lattice, with these alterations being retained in the final part, and controlled in their extent by the boundaries of the inclusion. A micrograph showing a larger-scale area of the microstructure with multiple AM regions visible is shown in Fig. 7. Since one of AM's chief strengths is its freedom of design paired with great structural precision, this means that *Add*FAST composites can benefit from a huge range of possible microstructures and architectures through AM, with excellent tailorability. The placement of the lattices into the powder mould also means that the wider part architecture can also be controlled, introducing AM morphologies and texture into specific areas and potentially designing site-specific properties into the part by adding the inclusion to different regions where certain responses are desired.

Another feature visible from these micrographs is the quality of the densification and interface between the two regions. In these conditions, both the matrix and the lattice region are of high density with only a few notable pores. The porosity of the *Add*FAST sample is given in Table 2, as well as the porosity of the DC lattice that was sectioned without powder addition or FAST treatment. This is also represented visually in Fig. 8. The level of density seen indicates a good suitability for service, but also importantly shows that the *Add*FAST process can naturally close internal porosity in the AM region. Being able to reduce a significant drawback of AM items as a natural stage of the process gives great potential to utilise the unique strengths of AM in these parts, without also introducing its

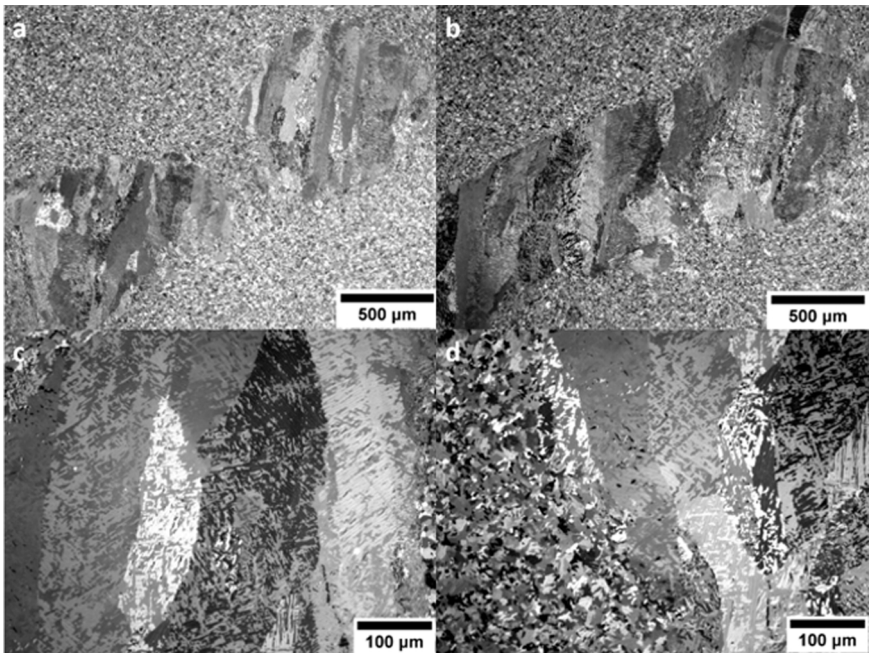

Fig. 6. Cross-polarised light micrographs of AddFAST samples sintered at 950 °C, using Ti-6–4 powder. a. and b. are at x5 magnification, c. and d. are at x20 magnification. The coarse grains seen originate from the AM strut and the fine grains originate from the FAST powder.

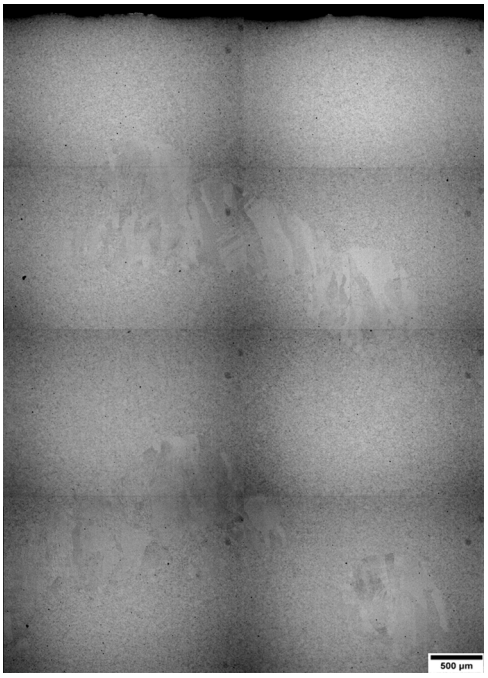

Fig. 7. Polarised light micrograph of the sample sintered at 950 °C showing a larger area of the microstructure, created by combining multiple adjacent small micrographs together.

Table 2
Porosity by %age area of the AddFAST sample in different regions of the microstructure, as well as in the untreated DC lattice.

Sample and Region of Microstructure	Porosity (%age by Area)	
	Average	Standard Deviation
***Add*FAST, overall**	0.02	0.01
***Add*FAST, matrix**	0.02	0.00
***Add*FAST, DC lattice**	0.04	0.03
Untreated DC Lattice	0.91	0.31

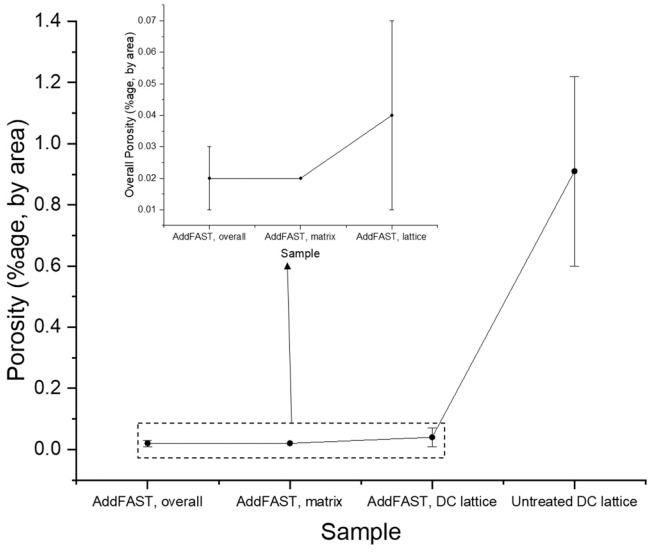

Fig. 8. Porosity by %age area of the AddFAST sample in different regions and the untreated DC lattice, represented visually.

well-known drawbacks. This could lead to a promising opportunity to increase the industrial application of AM, if the factors that usually inhibit use can be easily reduced this way. Additionally, the interface is consistently dense and void-free at all points in the microstructure. This means that as well as the intended complex microstructure being created and the architecture of the AM lattice retained in the final sample, the join between the two regions is also good-quality and suitable for load-bearing applications. As such, the potential complications of designing and performing further process stages to heal the interface are removed. This dense interface, as well as the resolution of the lattice micro- and macrostructure, was achieved with a straightforward process of placing the lattice into the powder mould and infiltrating the structure with powder. The lack of need for complex process stages, bonding additives or a more-complicated FAST treatment means that this process can achieve high-quality results while being simple and easy to perform at an industrial scale, although production of AM lattices will still be required.

The creation of this complex microstructure has the potential to introduce some novel behaviours. The introduction of coarse, columnar grains into a fine-grained microstructure would not be expected to increase mechanical strength; the more-probable effect, in fact, would be for that area of the part to lose strength. The AM addition, however, allows the distribution and extent of these grains to be finely controlled – the coarse grains would only be in the area occupied by the addition with a clear cut-off interface, as seen in Fig. 6. This means that the placement of AM additions in the part could create site-specific properties across its volume with very high control over the spatial distribution. Designing site-specific properties into the part can allow for local optimisation of performance, controlled property combinations and more-efficient structures where locally-adjusted behaviour reduces the need for over-designing the part as a whole. Reduced mechanical strength could be beneficial for modifying formability and functional grading of strength across the part; coarse grains could also create localised tailoring of creep strength. A preliminary investigation of the effect on mechanical properties in these parts is described in Section 3.5, as well as discussion of how it may be increased in future items. A controlled distribution of large, coarse grains throughout the part may also have significant results for functional properties such as thermal or magnetic behaviour. Grain size and grain aspect ratio is very significant for these behaviours, and a complex, controllable distribution of grain morphology with sharply-defined limits may allow for interesting, tailorable properties. Open lattice designs, employing AM's design freedom, would allow the additions to form an 'interpenetrating composite' where the grain structures are intertwined in continuous regions throughout the microstructure. This would cause their corresponding properties to affect the microstructure continuously in an integrated fashion with the fine-grained matrix, with the option of building monolithic addition parts if non-continuous combination would be desired. The ability to create this complex composite structure has potential to lead to a variety of novel and open-ended behaviours – however, it will also require a great deal of practical processing information in order to become a practically viable method for use in industry.

Fig. 6c. and d. also shows within the columnar grains of the *Add*FAST samples that a number of smaller sub-structures were also present. Although the long-distance alignment of the large grains from which they form is still distinctive, the cross-polarised light images shows that these structures are generally not of the same orientation as this background. To identify their origin, we took images of the microstructure of the original DC lattice prior to the FAST step. Micrographs of the lattice's microstructure are shown in Fig. 9. As well as the boundaries of the large columnar grains, the micrographs of the untreated lattice show a microstructure with many martensitic α' needles, which is expected from the cooling rates of the AM process. The transition from these into the sub-grain features seen in the 950 °C *Add*FAST sample directly correlates with α' martensite's transformation into laths on heating (Hui et al., 2020). We considered the possibility that these features are

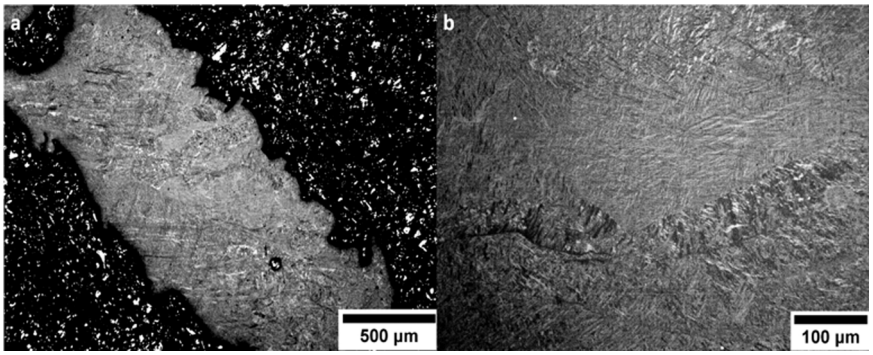

Fig. 9. Polarised light micrographs of the AM lattice microstructure. The black region in a. is mounting resin used for metallographic preparation.

recovered or recrystallised grains as the residual stress of the AM step was annealed out during the FAST heating cycle. However, they bore a closer resemblance to the (α + β) lath microstructure than they did to recovered grains in other titanium alloy samples (Popov et al., 2010); recrystallised grains would also be characteristically equiaxed in morphology compared to these elongated features. From this inspection, we have determined that the sub-grain features seen inside our columnar additive grains are transformed laths from the previous martensite microstructure, which occurs due to the FAST process cycle. If the long continuous grains were deemed to be concerning in an application where other aspects of this process would be useful, the ability to create a network of internal sub-grains in a simple manner may be a useful as a tool to give further control over the behaviour and properties of the part.

To see if the lattice's inclusion affected densification during FAST, the piston displacement against time data was taken from the machine's logs. This is compared against that of several 'Blank' samples of solely Ti-6–4 powder without lattice addition in Fig. 10. As not all of these samples were filled to identical initial height, the piston displacement was converted into compressive strain to allow data to be compared. We can see that the densification trend is the same in both *Add*FAST and normal samples, and that the compressive strain in the *Add*FAST runs is within a small range of that of the Blank samples. This gives us confidence that the presence of the lattice does not modify densification behaviour during the FAST process, which allows conventional predictions to be applied to this method as well.

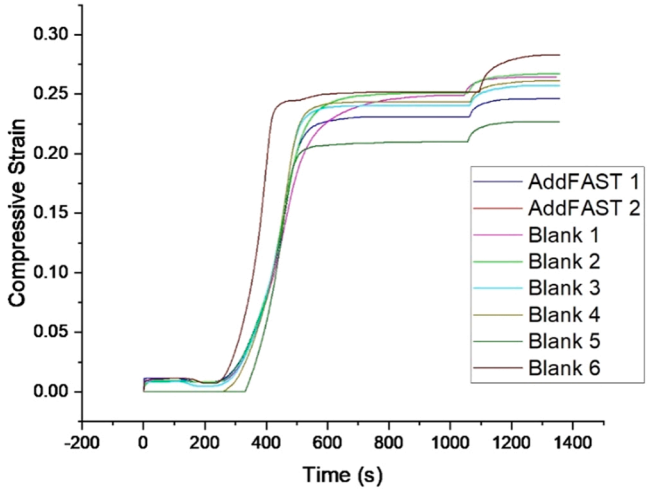

Fig. 10. Compressive strain vs. process time curves during FAST processing of the AddFAST samples and several 'Blank' samples containing only Ti-6–4 powder and no lattice addition.

3.2. Effect of processing parameters on AddFAST microstructure

A series of samples were fabricated using Ti-6–4 powder and the DC lattice to investigate the effect of dwell temperature on the resulting microstructure. These were sintered at 850 °C, 900 °C, 950 °C, 1000 °C and 1100 °C. Due to observations from these samples, a further sample was sintered at 1000 °C for 15 mins' dwell, rather than 10. The micrographs of these are shown in Fig. 11. The porosity of each sample, for the lattice and matrix regions and over the combined microstructure, is given in Table 3 and is represented visually in Fig. 12.

The effect on the composite's microstructure is clearly visible. The first and clearest result is that high-quality densification was not reached until 950 °C. In the 850 °C and 900 °C samples, an unacceptable level of porosity is easily visible in both the surrounding powder and the lattice region. This provides an important limit of viable process temperature for this alloy in these conditions, as well as the fineness of temperature difference that can have a significant effect on quality. It is also worth noting that in both the 850 °C and 900 °C samples the matrix was more porous, but pores still did not gather at or segregate to the interface. This gives further encouragement in the safety of these composites and the suitability of the interfacial join in fully-dense parts.

Secondly, the distinction between the two regions of the composite is easy to see in the samples processed at the subtransus temperatures of 850, 900 and 950 °C. Above Ti-6-4′s beta transus temperature of 980 °C, however, the clear change in structure starts to become lost. In fact, FAST samples processed at 1100 °C show that the clear and distinct regions of varying microstructure are no longer distinguishable, which means that the intended composite properties from the contrast between these regions are also lost. Heating the composites above the beta transus temperature effectively serves as a normalisation process, similar to the use of austenite transition to simplify the microstructure of steels. The 1000 °C sample with a dwell time of 15 mins was fabricated to try and capture this transformation mid-process; as it shows, the formation of new beta grains in these conditions causes the previous regions' boundary to lose distinction and breaks up the columnar AM morphology. After converting both prior regions to single-phase β titanium, the two regions then transform as one into (α + β) during cooling and lose their previous contrast. In the 1000 °C sample with a 10 min dwell, though, the distinct composite structure has not yet been lost; under these processing conditions normalisation did not proceed far enough to disrupt the microstructure, despite the dwell temperature being above beta transus. From these images, therefore, we have identified another important limit on the processing surface for this method: normalisation will destroy the desired grain architecture, and so processing above the beta transus must only be performed for very limited time/excess temperature so that the beta transformation does not have time to progress far enough. By extension we can determine that the *Add*FAST method should be applied with discretion to parts that would otherwise require high-temperature homogenisation treatment. Whether modifying the pressure or heating rate of FAST can improve

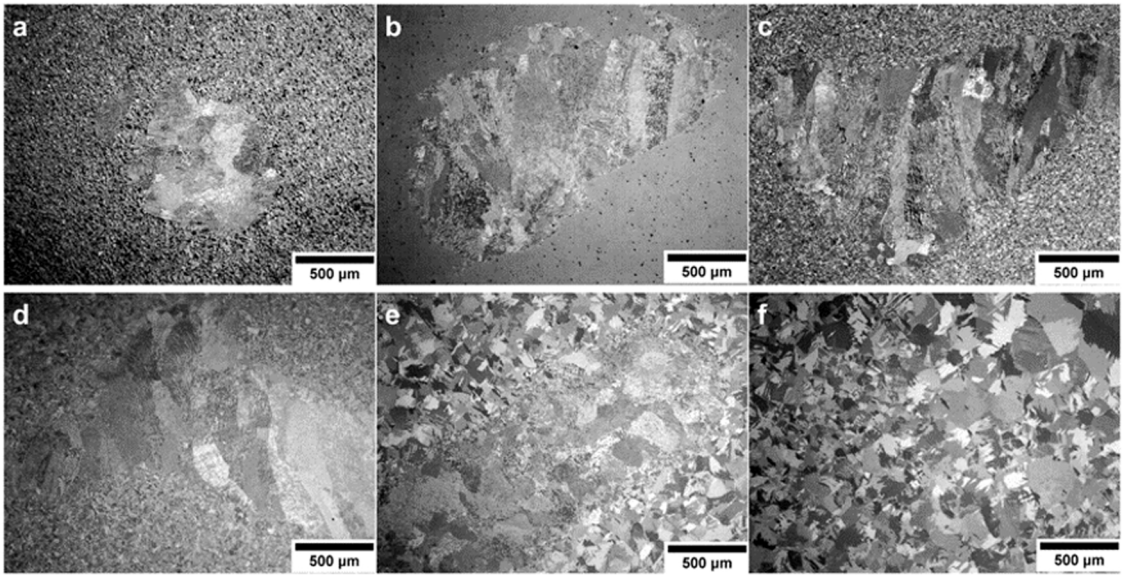

Fig. 11. Polarised light micrographs of AddFAST samples sintered at a. 850 °C, b. 900 °C, c. 950 °C, d. 1000 °C 10 mins, e. 1000 °C 15 mins and f. 1100 °C.

Table 3
Porosity by %age area of the samples produced at different processing conditions, including the two regions of the microstructure and the microstructure overall. As the different regions are not distinct in the 1100°C sample, this area of the table is omitted.

Process Conditions	Overall (%age by area)		Matrix Region (%age by area)		DC Lattice Region (%age by area)	
	Average	Standard Deviation	Average	Standard Deviation	Average	Standard Deviation
850 °C	7.49	3.67	6.26	1.61	2.74	1.39
900 °C	2.37	1.76	3.03	2.03	0.26	0.33
950 °C	0.03	0.01	0.02	0.00	0.04	0.03
1000 °C, 10 min	0.05	0.04	0.03	0.02	0.08	0.06
1000 °C, 15 min	0.05	0.05	0.03	0.01	0.01	0.09
1100 °C	0.04	0.01				

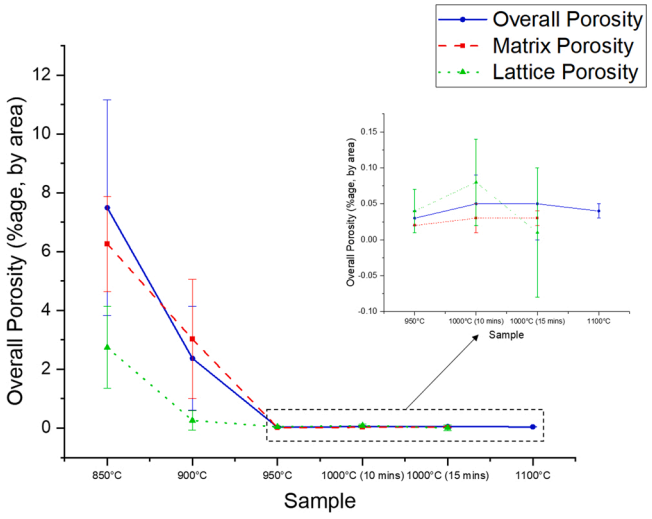

Fig. 12. Porosity by %age area of the samples produced at different processing conditions, represented visually.

sub-transus densification in those cases will be part of future work on this technique. With the lack of density below 950 °C identified previously, these results establish a simple processing window for Ti-6-4 in these conditions – a useful tool for considering application of this technique to the premier titanium alloy. Crucially, though, the fact that beta normalisation will remove the intended structure is a general guideline that will likely apply to other alloy compositions as well – an extremely important tool for increasing and broadening application of this method if proven true.

After identifying the significance of the beta transformation in the process, we investigated the effect of processing *Add*FAST samples at lower temperatures but for extremely long dwell times, well beyond those required by standard production. Samples were produced at dwell temperatures of 850 °C and 900 °C for dwell times of 30, 45, 60 and 75 mins. These were all fabricated with Ti-6-4 powder and used the BCC lattice design, as described in Section 2.2. All other processing parameters were the same as described previously. Since these samples had been fabricated after the samples that contained the BCC lattice that are discussed in Section 3.5, we were already confident that this structure could be successfully infiltrated throughout by powder and densified to a high quality of matrix and interface by the same method. Our intention, therefore, was to apply the method to our finer complex samples with the knowledge that this complexity would not affect the densification (and result quality) by itself. The microstructures of the samples in this set are shown in Fig. 13.

In all of the samples processed this way, we can clearly see the distinct composite structure. The two regions and their individual grain structures are clear and easy to identify, as well as still possessing a dense, high-quality interface. The shape of the regions and structure of the lattice addition is also retained in all of these parts. Although we found that the beta transformation was destructive for our part, and so that processing around the beta transus temperature was a potential risk, processing at these lower temperatures for longer times was safe and lead to clear retention of the parts' micro- and macrostructure even when dwell times vastly exceeded what would be economical from a

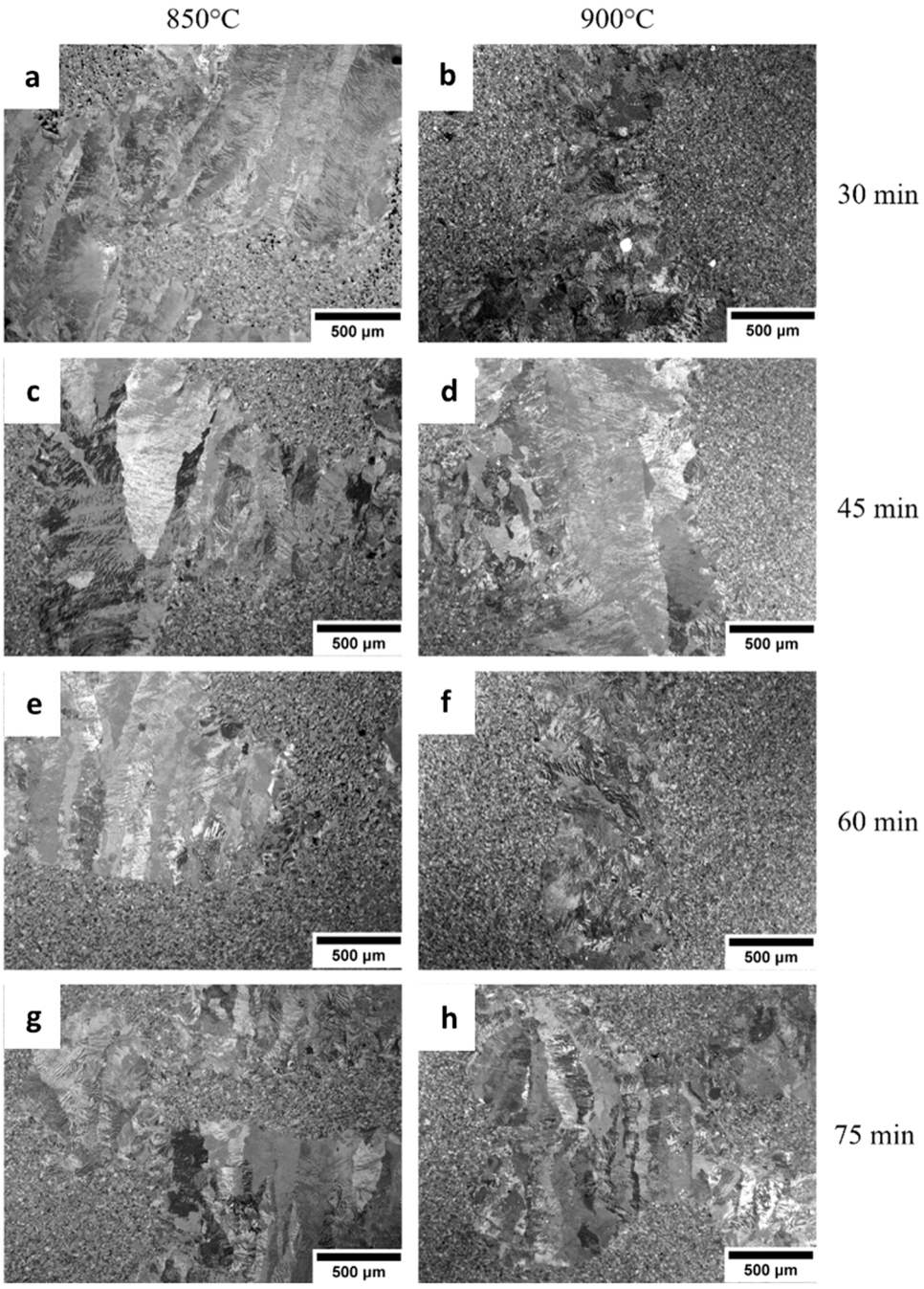

Fig. 13. Polarised light micrographs showing the microstructure of AddFAST samples, processed at 850 and 900 °C for dwell periods between 30 and 75 mins.

process standpoint. This identifies the dwell temperature as by far the more important parameter for retaining the composite structure in *Add*FAST, with an excess increase in time having a much smaller effect than an increase in process temperature. Only once the samples begin to approach their beta transus does processing time become more significant, as shown with the two 1000 °C images in Fig. 13. However, almost all of the samples processed this way also showed some significant pores surviving at the end of the process, with porosity only reduced to acceptable levels in the 900 °C 60 min and 75 min samples (Fig. 8f and h). Although using lower temperatures and very long dwell times could be a viable way to consolidate powders that would normally be hard to densify at sub-transus temperatures, these results indicate that the time may have to be drastically increased to achieve satisfactory results and that some temperatures (850 °C, in this case) may be ineffective options regardless of dwell period. Identifying the relative significance of process parameters in *Add*FAST will be extremely important for confident application and gaining the understanding needed to be able to this method in industry. As such, continuing to develop our understanding of the effect of different parameters will be crucial as the process and its application matures, including whether it remains the case when using alloys of other systems.

It should also be noted that the highest-quality microstructures (the 900 °C 60 min and 75 min samples, Fig. 8f and h) also show that there was no limit on the degree of densification achievable caused by the use of the BCC lattice in these samples rather than the DC lattice. The finer structure with smaller open pores was still fully infiltrated and densified with a high quality interface, as the DC lattice samples had been. This demonstrates that the BCC lattice does not affect the degree of infiltration and so allows these results to be comparable to the quality of the DC results, as mentioned previously – if infiltration degree had been

affected, these highest-quality results would not have been achievable. This also shows generally that the *Add*FAST method can successfully apply to smaller addition structures with smaller openings and complex designs. Investigation of the degree of size mismatch between powder and opening size that makes infiltration incomplete via. this method will be part of future research work.

As well as the retention of the titanium-titanium composite structure as a whole, we also looked at how the lower temperature and longer dwell time affected the structure within the AM regions. In the 850 °C samples, the internal columnar grains can still clearly be seen in all samples, even after 75 mins of processing (Fig. 8g). At this temperature, even extremely lengthy process times did not remove the complex microstructure. In the 900 °C samples, the columnar grains were easy to identify throughout the 45 and 75 min samples (Fig. 8d and h), while in the 30 and 60 min samples (Fig. 8b and f) they were clear in some locations, possible to identify in others and almost indistinguishable in others. Since the 45 and 75 min samples still showed the internal structure clearly and unambiguously, it does not appear that there was a critical process time above which the grain morphology was lost when FAST processing at 900 °C – the difference in structural consistency for the 30 and 60 min samples must be due to another set of factors. The 30 and 60 min samples, as mentioned, did contain some areas where the columnar grain structure could be identified easily. As such, we would say that processing at these lower temperatures allows the survival of the previous columnar morphology even after extremely-long dwell periods, rather than transforming into a different structure with different behaviour that would complicate predictions. However, the variance seen in the 900 °C 30 and 60 min samples should still be noted, and further testing may be appropriate to identify if this continues to be seen, which conditions it happens under and what if any effect it has on performance. Fundamentally, we would say that the columnar grains and their sub-grain features have survived in these conditions, as well as the broader composite structure.

The size of the grains within the AM regions of these samples, including the ones processed for long dwell periods, were measured by the Linear Intercept Method. Our measurements found that there was no clear trend of grain size with process parameters. The grain sizes in the AM regions were insensitive to FAST treatment, as long as they were not removed by normalisation. From this we found that rather than attempting to tailor grain size by the design of the FAST process, efforts to design the grain morphology of the *Add*FAST composite should be directed at process control in the AM fabrication stage. The results of this control will then be generally unaltered by subsequent processing.

While considering the potential for different FAST parameter combinations to produce parts, we determined the energy use in the FAST process for each sample. If two processes produced similar parts but required significantly different amounts of energy, this would help inform industrial processing and choice of production route. Energy use for each run was determined by using the data logs of the FAST machine. Summing the power used at each one-second step gave the total energy use for all steps in the heating and dwell sections of the process. Energy required for water-cooling of the electrodes, which would be greater at higher temperatures, could not be tracked by our data-logging equipment. However, this level of energy is likely to be very small compared to the energy requirement of the FAST densification processes, even at higher temperatures, and so has been deemed safe to omit from our analysis. The graphite felt jacket, used with all samples, significantly reduces thermal loss as described by Laptev et al. (2018); for this insulation arrangement Laptev's work also indicates that its insulating effect should be similar for all temperatures. Therefore, even in cases where it was not used the relationship between values should be consistent. More-complex insulation arrangements may lead to a differing relationship between values at different temperatures, but these arrangements are not standard practice. A contour plot of the process energy and some of the resulting microstructures is shown in Fig. 14.

Fig. 14 clearly shows that the energy use in processing depends far more strongly on process time than it does on temperature. Although there is a predictable increase in energy needed when processing at higher temperatures, this was revealed to be very small compared to the energy increase of processing for longer dwell periods. This has major consequences for choice of FAST processing conditions, as the two approaches that produced suitable quality of microstructure were 950/1000 °C for 10 min and 900 °C for 60/75 min. However, the 900 °C approach uses 3.4–4.5 times the amount of energy, and so incurs 3.4–4.5 times the cost in energy charges, as the 950/1000 °C approach to produce parts of equal quality. From this, we can see and can recommend for future production that although *Add*FAST parts can be produced by processing at low temperatures for a long dwell period, it is far more cost-effective to produce the parts at higher temperature for a shorter dwell time. Such a method would also allow for a higher throughput, providing another crucial economic advantage. This also gives direction to investigations of *Add*FAST process surface, as the priority should evidently be to find process temperatures that give high-quality results in a shorter dwell time. This is a guideline that, crucially, can be applied to the development and use of other alloys as well as Ti-6-4 – though precise values will vary with the alloy under investigation, *Add*FAST processes to produce the same part are likely to be cheaper to operate as shorter, higher-temperature runs than longer, lower-temperature methods.

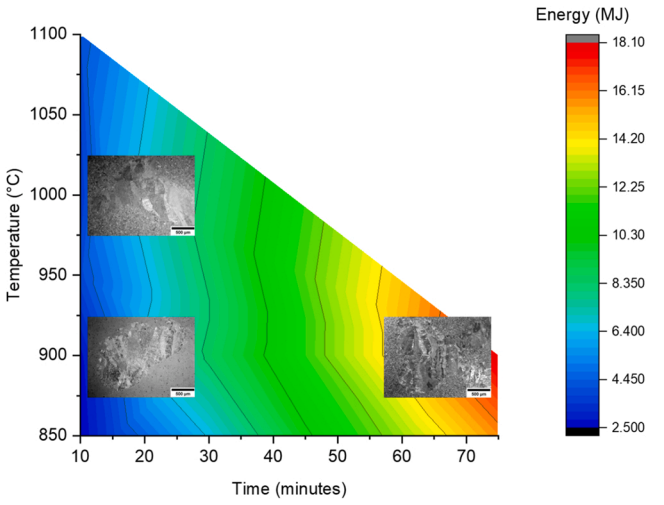

Fig. 14. Contour plot of the energy requirements of different FAST process parameters, including resulting microstructures from different conditions.

As well as investigating the process surface of variation in time and temperature, future work on the effect of process parameters should also address variation (chiefly the increase) of applied pressure and heating rate during FAST. These can also improve densification with comparatively-low increase in the energy requirement, particularly higher heating rates that can trigger densification mechanisms such as grain boundary diffusion. These may be of particular importance when considering other alloy compositions that do not sinter as effectively below their beta transus as Ti-6–4.

3.3. *Effect of AddFAST process on texture*

As well as grain morphology, another important factor of adding AM structures to the sintered matrix is the complexity of micro-texture. As discussed in the introduction, the nature of AM fabrication affects the texture and grain orientations of the part as well as the morphologies of the growing grains, increasing the process' effect on properties. In the polarised light micrographs in Fig. 6, the contrast indicates that each of the large columnar AM grains has a distinctive orientation visible throughout their height, vastly different to the mixed texture of the surrounding powder grains. EBSD analysis of these samples, shown in

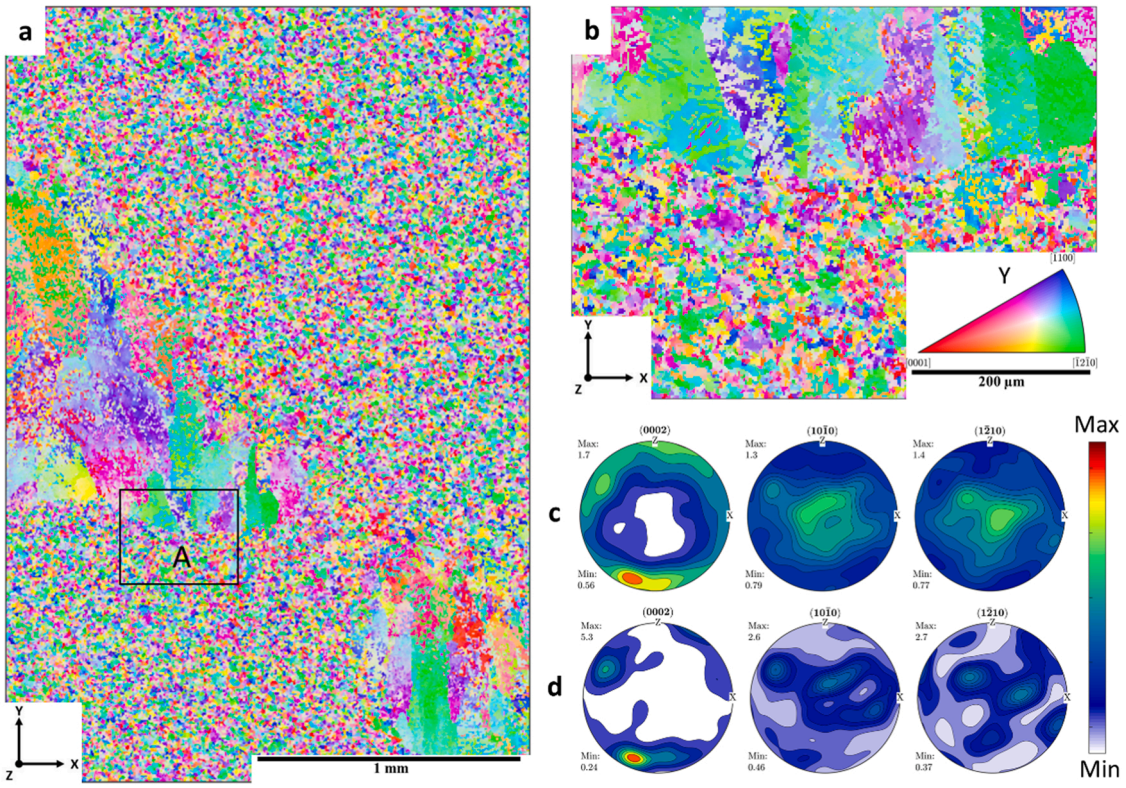

Fig. 15. Texture analysis performed in the 950 °C AddFAST sample showing (a) IPF-Y orientation maps covering a large area of 2 × 4 mm^2, (b) high resolution IPF-Y orientation maps at location A and pole figure plots of (c) the overall texture of the sample and (d) texture of the lattice region only. The Y direction is equivalent to the consolidation direction during sintering.

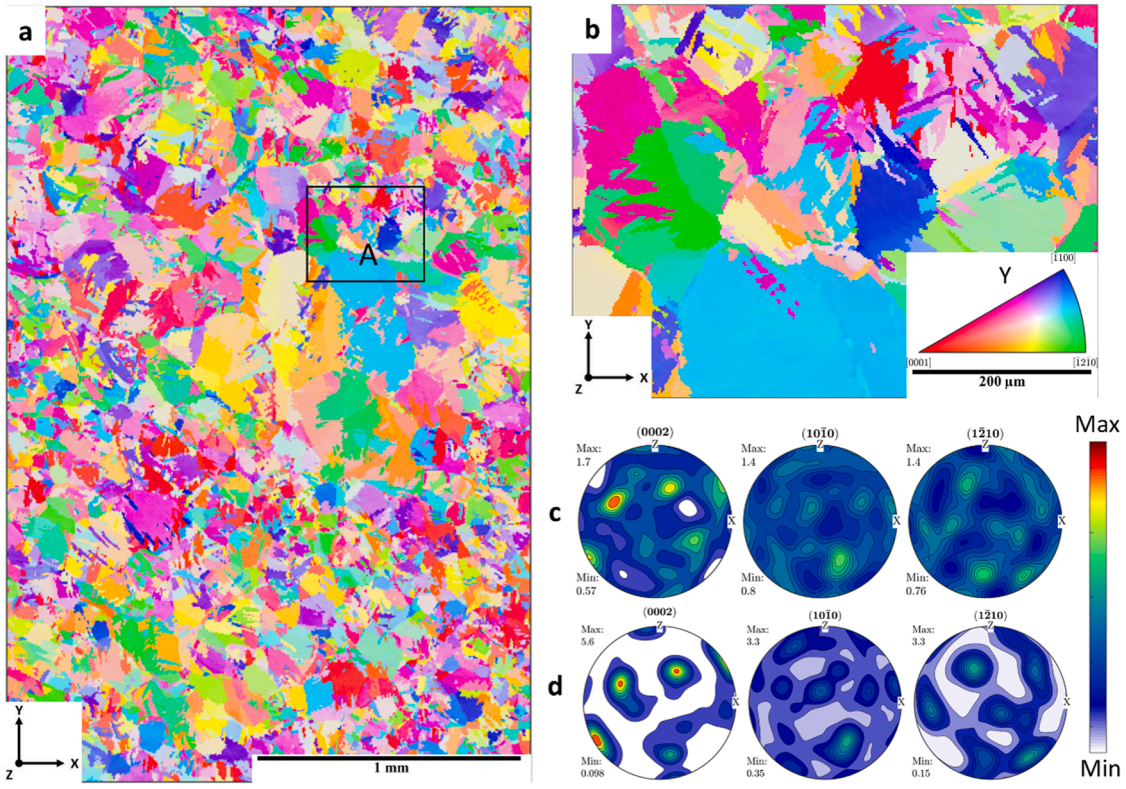

Fig. 16. Texture analysis performed in the 1100 °C AddFAST sample showing (a) IPF-Y orientation maps covering a large area of 2 × 4 mm^2, (b) high resolution IPF-Y orientation maps at location A and pole figure plots of (c) the overall texture of the sample and (d) texture of the lattice region only. The Y direction is equivalent to the consolidation direction during sintering.

Fig. 15, was used to gain a more-precise mapping of the grain texture.

The EBSD mapping clearly reveals the effect of the AM additions on the overall texture of the sample. The grains in the lattice regions show large areas of continued background orientation, strongly contrasting to the random texture of the surrounding matrix (Fig. 15a and b). The pole figure plots of the whole data set (Fig. 15c) show a weak compression texture commonly observed in FAST-processed material, with a slight variation inherited from the texture observed in the lattice (Fig. 15d). The controlled layout of texture variation, following the shape of the additive regions, is also clearly visible. This means that as well as a complex arrangement of different grain sizes and shapes, the *Add*FAST technique can be used to create a complex arrangement of texture throughout the composite as well. The open-ended design possibilities of Additive Manufacturing again mean that the spatial distribution of these different textures can be precisely controlled by the engineer, allowing for tailoring of novel properties for both mechanical and functional applications. As with the differing grain morphologies, the ability to place the lattice into the powder mould can also allow for creating these complex texture distributions in certain regions of the part, leading to the potential for site-specific properties.

EBSD analysis was used with the sample processed at 1100 °C to investigate if the AM regions' texture was retained even if the grain structure had been lost. The results are shown in Fig. 16. Overall, the complex contrast in texture appears to have been lost in the 1100 °C sample in the same way that the microstructural contrast was lost. This further reiterates the importance of preventing beta normalisation in these parts, as it removes both of the complex arrangements we may intend to create.

There is, in Fig. 16, a visible area of large grains just below Location A that resemble an area of the prior lattice. This morphology would be unlikely to occur naturally from grain growth in the FAST process, and so indicates that even in these conditions it is still possible for some lattice features to survive. However, even with these features' presence, the majority of the microstructure is still one of large, normalised grains. This means that where AM grain features are retained, they provide much less contrast to the surrounding microstructure due to both the smaller size of those AM areas and the growth of the surrounding 'matrix' grains. On this basis we would say that our previous assessment of extensive supertransus treatment being destructive to the *Add*FAST composite's function is still true, even when variations in the temperature distribution allow some grains to still survive.

3.4. Effect of matrix powder composition

A set of *Add*FAST samples with the DC lattice were fabricated using a powder matrix of near-α type alloy Ti-6-2-4-2 powder, as opposed to the Ti-6-4 powder used in the rest of this study. This was intended as a brief investigation of the potential to produce *Add*FAST parts with two alloys of different composition. Ti-6-2-4-2 powder was used to examine the effect of combining a near-α alloy with the (α + β) alloy in the lattice; Ti-5-5-5-3 powder was intended to examine the effect of a near-β alloy powder, but resource availability meant this could not be achieved in this work. Sintering was performed at 950 °C for a dwell time of 10 mins, and all other parameters were as described in Section 2.3. Micrographs of the sample are shown in Fig. 17.

As with the previous results, the Ti-6-2-4-2 matrix sample clearly retains the visible distinction between the powder and AM regions. The crucial composite structure and variation of grains in the two regions is also retained, and the interface between the two regions is again dense and indicates suitability for service. This is a very significant result, as it shows that fundamentally the *Add*FAST technique can be applied to both similar and dissimilar alloy composition pairings and produce the desired microstructure in both cases. The ability to combine different alloys and produce the same quality of composite architecture greatly multiplies the possibilities for this technique. Use of AM to create the additions, as well creating a complex grain morphology arrangement, will allow composites to be created with small, well-defined additions that could lead to controlled site-specific properties throughout as described before; the AM process can also allow for fine, freeform addition designs that will have an impact on resulting properties beyond the combination of materials. In this case, dissimilar alloy pairing was demonstrated with two Ti alloys; however, there is no evident reason at this stage why *Add*FAST cannot be used to combine alloys of entirely separate base systems, opening application opportunities even further.

However, there are also important practical issues. Although the composite structure – clear, distinguished regions of varying grains with a dense interface – is of excellent quality in the 6-2-4-2 sample, its matrix also contains a nontrivial level of porosity. This occurred despite being sintered in conditions that produced a highly-dense 6-4 matrix. Further sintering, at either increased time or temperature, would be needed before this part could be used in service. This was determined to be due to the dominant mechanism in micrometric-powder sintering being power-law creep (Olevsky and Froyen, 2006). Ti-6-2-4-2′s higher creep strength compared to Ti-6–4 slows mass transfer in the sintering process, leading to the porosity observed from the same process conditions. As work continues on combining different materials in *Add*FAST, identifying important parameters for successful sintering will be useful for predicting materials that require adjusted process conditions to complete densification without having to test each case individually. This result also shows the importance of tailoring *Add*FAST parameters with the less-sinterable alloy of the pair in mind.

3.5. Effect of AddFAST process on mechanical properties

The stress-strain curves of sintered *Add*FAST samples containing the BCC lattice design are shown in Fig. 18a. These were gathered from room-temperature compression, as described in Section 2.4. This forms part of an ongoing investigation of the effect of the lattice structure on mechanical properties, with a focus on lattice designs that will let us investigate particular features and behaviour of the original structure and their potential effect on the *Add*FAST part. As the planned lattices for this investigation have been chosen for these purposes of investigating certain features, the DC lattice is not part of our mechanical testing set. All of the compression tests ended with the samples

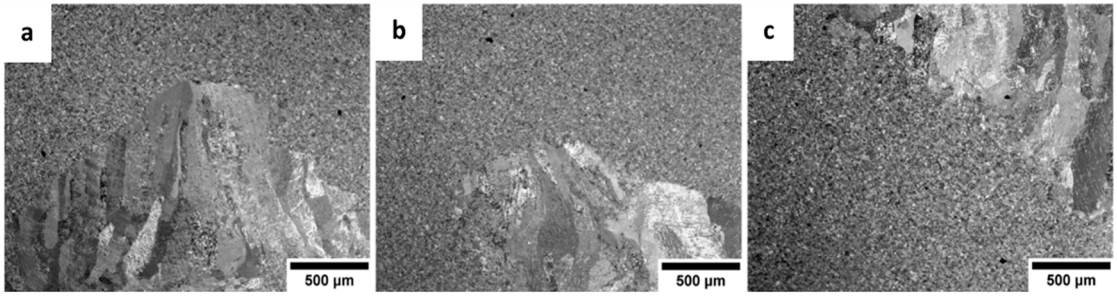

Fig. 17. Polarised light micrographs of AddFAST samples with a Ti-6–2–4–2 matrix, sintered at 950 °C.

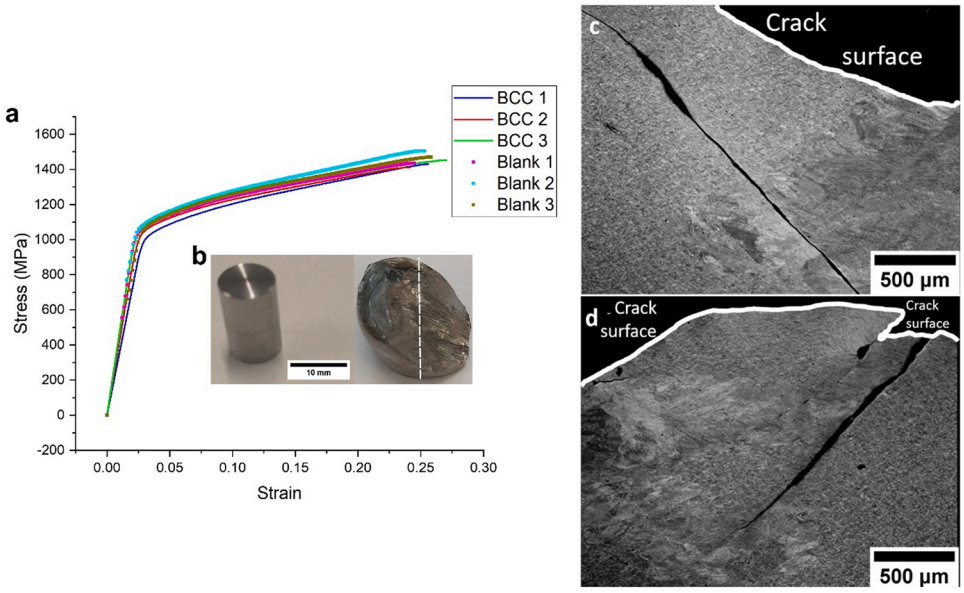

Fig. 18. a. shows the stress-strain curves of AddFAST samples produced with the BCC lattice, tested in room temperature compression. 'Blank' refers to samples that consisted only of FAST-processed Ti-6–4 powder and no lattice. b. shows an example of a compression sample before testing and a fractured half of a sample post-compression, with a white dashed line to show the approximate area of the cut used to acquire through-thickness micrographs. It should be noted that this is an example of such a sample and is not the same as the one used to acquire said micrographs for this figure. c. and d. show through-thickness polarised light micrographs of the fractured sample, showing its deformed microstructure.

fracturing, an example of which is shown in Fig. 18b. These fractured samples were sectioned through their thickness, followed by polishing and light microscopy to identify any significant fracture behaviours within the microstructure. Example through-thickness micrographs are shown in Fig. 18c and d, with the main crack (whose surface is marked) coming diagonally out of the page.

The goal of this testing was not to establish a conclusive value for the flow stress of these samples, but rather to understand the effect that the presence of the AM lattice and its design features had on the part under compressive loads. As shown in Fig. 18a, however, almost no difference in mechanical properties was seen. Despite the presence of large columnar grain regions from the AM, the strength of the *Add*FAST samples was very similar to that of samples containing only FAST-processed powder. This consistency of properties means that the *Add*-FAST parts can still be used reliably in load-bearing applications similar to those of conventional FAST items. Microstructural interfaces often create a potential risk of weakness in many parts, acting under load as a point of delamination or crack nucleation. These results, however, show that there is no deterioration in strength from introducing the lattice to these parts. Fig. 18c. and d. show that the main crack through the part was unaffected by the composite and its interface, which was even true of the microcracks that formed alongside the main failure. This very important result shows the potential hazard and application-limiting weakness of the interface does not affect these *Add*FAST parts, which removes a major concern that would potentially limit the process from use with load-bearing items. Consistent mechanical performance means that this process can be used for parts of the same requirements and for the same applications as normal FAST-processed parts, and that the complex microstructure and texture can be utilised (eg. for functional properties) with much less prior research required on mechanical safety. Overall this is a very important result for confirming the applicability and practical suitability of this method, as well as demonstrating its technical effects.

In these cases, the AM lattice structures only occupied a very small volume fraction of the sample – approximately 18 %. In this proportion, it is possible that the large AM grains may not have a major impact on the overall part's strength, and future work will include investigating whether a higher volume fraction of the larger columnar grains starts to create a more pronounced effect on the part under compressive loads. If this is successful, this creates the possibility of using the AM addition to tailor the mechanical response of the part and make further use of the freeform ability to design complex AM parts, as well as introducing inclusions in specific areas of the part for site-specific behaviour (one of the behaviours also discussed in Section 3.1). The effect of the lattice on mechanical properties could also be enhanced by changing and combining the alloy compositions, which could benefit from AM's freeform design potential to create complex, precise structures that affect behaviour as well as the combination of composite materials. Surface-treating the lattice before addition could also lead to its surface acting as a load-bearing internal skeleton of the composite, which could also benefit greatly from the ability to create complex AM designs by this process in nearly any desired structure for achieving various properties.

4. Conclusion

In this paper, a method for creating parts with complex composite microstructures by combining AM and FAST has been investigated. The microstructures were found to contain distinct regions of differing grain morphology and size that correspond to characteristic AM and FAST-produced features. The AM regions also contained numerous ($\alpha + \beta$) sub-grains and were of high density, as was the interface between the regions. The FAST dwell temperature was found to have a much greater effect on the final composite microstructure than the process time, especially the β-phase transformation which destroyed the composites by normalising out their complex microstructure. The samples also showed a complex composite arrangement of micro-texture as well as grain morphology, with this arrangement also being removed by β-phase transformation. Fundamental results demonstrated that this method can be applied to a mixture of alloy compositions in the separate regions of the part. The mechanical properties of these composites were found to be similar to conventional FAST-produced parts and the microstructure remained cohesive under severe deformation.

Funding

This work was funded by the Engineering and Physical Sciences Research Council (United Kingdom) through the Future Manufacturing Hub in Manufacture using Advanced Powder Processes (EP/P006566/1). We acknowledge the Henry Royce Institute for Advanced Materials (United Kingdom), funded through EPSRC grants EP/R00661X/1, EP/P02470X and EP/P025285/1. The funding sources had no involvement in the design or performance of the study, the writing of the report or the decision to submit the work for publication.

CRediT authorship contribution statement

Cameron Barrie: Methodology, Validation, Investigation, Data Curation, Writing – Original Draft, Visualization. **Beatriz Fernandez-Silva:** Investigation, Visualization, Writing – Review and Editing. **Rob Snell:** Resources. **Iain Todd:** Conceptualization, Supervision, Project Administration, Funding Acquisition. **Martin Jackson:** Conceptualization, Writing – Review and Editing, Supervision, Project Administration, Funding Acquisition.

Declaration of Competing Interest

The authors declare that they have no known competing financial interests or personal relationships that could have appeared to influence the work reported in this paper.

Data availability

Data will be made available on request.

Acknowledgements

The authors would like to thank Ben Thomas and Simon Graham for help with FAST work and Dean Haylock for assistance with compression testing.

References

Al-Bermani, et al., 2014. The origin of microstructural diversity, texture, and mechanical properties in electron beam melted Ti-6Al-4V. Metall. Mater. Trans. A: Phys. Metall. Mater. Sci. 45 (*4*). P.2142-2151. **Self-citation**.

Beynet et al., 2019a, Method for manufacturing a part of complex shape by pressure sintering starting from a preform, WO2020070107A1, WIPO (PCT).

Beynet et al., 2019b, Method for manufacturing a part of complex shape by pressure sintering starting from a preform, EP3860785B1, European Patent Office.

Beynet et al., 2019c, Method for producing a counter-form and method for manufacturing a part having a complex shape using such a counter-form, WO2020070133A1, WIPO (PCT).

Bowden and Peter, (2012) Near-Net Shape Fabrication Using Low-Cost Titanium Alloy Powders, U.S. Department of Energy, Oak Ridge National Laboratory.

Chougrani, et al., 2017. Lattice structure lightweight triangulation for additive manufacturing. Comput. Aided Des. 90, 95–104.

Decker, et al., 2016. Synthesis and mechanical properties of TiAl particle reinforced Ti-6Al-4V. Mater. Sci. Eng. A. 674, 361–365.

Dong, et al., 2016. Understanding the spark plasma sintering from the view of materials joining. Scr. Mater. 123, 118–121.

Duda, Raghaven, 2016. 3D Metal Printing Technology. IFAC-PapersOnLine 49 (*29*), 103–110.

Dutta, Froes, 2017. The additive manufacturing (AM) of titanium alloys. Met. Powder Rep. 72 (*2*), 96–106.

Eriksson, et al., 2005. Fast densification and deformation of titanium powder. Powder Metall. 48 (*3*), 231–236.

Gong, et al., 2014. Analysis of defect generation in Ti-6Al-4V parts made using powder bed fusion additive manufacturing processes. Addit. Manuf. 1, 87–98.

He, et al., 2012. Temperature-gradient joining of Ti-6Al-4V alloys by pulsed electric current sintering. Mater. Sci. Eng. A. 535, 182–188.

Hernández-Nava et al., 2016, A study on the mechanical properties of micro-truss Ti-6Al-4V materials fabricated by Electron Beam Melting, Thesis, University of Sheffield, P.45–46. Self-citation.

Hernández-Nava, et al., 2019. Additive manufacturing titanium components with isotropic components with isotropic or graded properties by hybrid electron beam melting/hot isostatic pressing powder processing. Sci. Rep. 9 (*1*). P.1-11. **Self-citation**.

Huang and Yeong, 2018, Laser re-scanning strategy in selective laser melting for part quality enhancement: A review. In: Chua, C. K., Yeong, W. Y., Tan, M. J., Liu, E., Tor, S. B. (Eds.), Proceedings of the International Conference on Progress in Additive Manufacturing, Singapore, P.413–419.

Hui, et al., 2020. Study on transformation mechanism and kinetics of α' martensite in TC4 alloy isothermal aging process. Crystals 10 (*3*). Article no. 229.

Klein, Schwarzer, 2010. Texture analysis with MTEX – free and open source software toolbox. Solid State Phenom. 160, 63–68.

Kozlík, et al., 2021. Interface of a Al6061/Ti composite prepared by field assisted sintering technique. Metals 11 (1), 73.

Laptev, et al., 2018. Enhancing efficiency of field assisted sintering by advanced thermal insulation. J. Mater. Process. Technol. 262, 326–339.

Lee, et al., 1997. Factors determining crystal orientation of dendritic growth during solidification. Mater. Chem. Phys. 47, 154–158.

Levy, et al., 2018. Ultrasonic additive manufacturing of steel: method, post-processing treatments and properties. J. Mater. Process. Technol. 256, 183–189.

Liashenko, et al., 2020. Processing of hybrid structure by partial sintering of Ti-6Al-4V powder into EBM lattices. Cherkasy Univ. Bull. Phys. Math. Sci. 1 (*1*), 16–25.

Martin, et al., 2016. Coupling electron beam melting and spark plasma sintering: a new processing route for achieving titanium architectured microstructures. Scr. Mater. 122, 5–9.

Molaei, Fatemi, 2019. Crack paths in additive manufacturing metallic materials subjected to amultiaxial cyclic loads including surface roughness, HIP, and notch effects. Int. J. Fatigue 124 (March), 558–570.

Mumtaz, Hopkinson, 2010. Selective laser melting of Inconel 625 using pulse shaping. Rapid Prototyp. J. 16 (*4*), 248–257.

Nguyen, 2021. Design for additive manufacturing of functionally graded lattice structures: a design method with process induced anisotropy consideration. Int. J. Precis. Eng. Manuf. - Green. Technol. 8 (*1*), 29–45.

Olevsky, Froyen, 2006. Constitutive modeling of spark-plasma sintering of conductive materials. Scr. Mater. 55 (*12*), 1175–1178.

Pope et al., 2019, FAST-DB: A novel solid-state approach for diffusion bonding dissimilar titanium alloy powders for next generation critical components, J. Mater Process. Tech., **269**, P.200–207. **Self-citation**.

Popov, et al., 2010. Effect of heat-treatment conditions on structural and phase transformations in a two-phase α + β titanium alloy subjected to thermomechanical treatment. Phys. Met. Met. 109 (*6*), 655–661.

Querin, et al., 2000. Computational efficiency and validation of bi-directional evolutionary structural optimization. Comput. Methods Appl. Mech. Eng. 189 (*2*), 559–573.

Rahmani et al., 2019a, Wear resistance of (Diamond-Ni)-Ti6Al4V gradient materials prepared by combined selective laser melting and spark plasma sintering techniques, Adv. Tribol., Article no. 5415897.

Rahmani, et al., 2019b. Modelling of impact-abrasive wear of ceramic, metallic, and composite materials. Proc. Est. Acad. Sci. 68 (*2*), 191–197.

Rahmani, et al., 2019c. Comparison of mechanical and antibacterial properties of TiO2/Ag ceramics and Ti6Al4V-TiO2/Ag composite materials using combined SLM-SPS techniques. Metals (Basel) 9 (*8*). Article no. 874.

Rahmani, et al., 2019d. Mechanical behavior of Ti6Al4V scaffolds filled with CaSiO3 for implant applications. Apply. Sci. 9 (18). Article no. 3844.

Rahmani et al., 2019e, Selective laser melting of diamond-containing or postnitrided materials intended for impact-abrasive conditions: experimental and analytical study, Adv. Mater. Sci. Eng., Article no. 4210762.

Rahmani, et al., 2020. Perspectives of metal-diamond composites additive manufacturing using SLM-SPS and other techniques for increased wear-impact resistance. Int. J. Refract. Met. Hard Mater. 88. Article no. 105192.

Rozvany, et al., 1992. Generalized shape optimization without homogenization. Struct. Optim. 4, 250–252.

Suárez, et al., 2012. Challenges and Opportunities for Spark Plasma Sintering: A Key Technology for a New Generation of Materials. In: Ertuğ, B. (Ed.), Sintering Applications. IntechOpen, Istanbul, pp. 319–342.

Torresani, et al., 2023. Fabrication of powder components with internal channels by spark plasma sintering and additive manufacturing. J. Eur. Ceram. Soc. 43 (*3*), 1117–1126.

Wei, et al., 2015. Evolution of solidification texture during additive manufacturing. Sci. Rep. 2015 (5). Article No. 16446.

Weston, Jackson, 2017. FAST-forge – a new cost-effective hybrid processing route for consolidating titanium powder into near net shape forged components. J. Mater. Process. Tech. 243, 335–346 (Self-citation).

Yang, et al., 2021. Fatigue properties of Ti-6Al-4V Gyroid graded lattice structures fabricated by laser powder bed fusion with lateral loading. Addit. Manuf. 46. Article no. 102214.

Zhang, et al., 2022. Mechanical responses of sheet-based gyroid-type triply periodic minimal surface lattice structures fabricated using selective laser melting. Mater. Des. 214. Article no. 110407.